

Plasmonic solar cells

K.R. Catchpole,^{1,2*} and A. Polman,¹

¹FOM Institute for Atomic and Molecular Physics, Kruislaan 407, Amsterdam, The Netherlands

²Centre for Sustainable Energy Systems, Australian National University, Canberra, ACT 0200, Australia

*Corresponding author: kylie.catchpole@anu.edu.au

Abstract: The scattering from metal nanoparticles near their localized plasmon resonance is a promising way of increasing the light absorption in thin-film solar cells. Enhancements in photocurrent have been observed for a wide range of semiconductors and solar cell configurations. We review experimental and theoretical progress that has been made in recent years, describe the basic mechanisms at work, and provide an outlook on future prospects in this area.

©2008 Optical Society of America

OCIS codes: (350.6050) Solar energy; (240.6680) Surface plasmons; (040.5350) Photovoltaic

References and links

1. J. Müller, B. Rech, J. Springer, and M. Vanecek, "TCO and light trapping in silicon thin film solar cells," *Solar Energy* **77**, 917-930 (2004).
2. J. Meier, S. Dubail, S. Golay, U. Kroll, S. Faÿ, E. Vallat-Sauvain, L. Feitknecht, J. Dubail, and A. Shah, "Microcrystalline silicon and the impact on micromorph tandem solar cells," *Sol. Energy Mater. Sol. Cells* **74**, 457-467 (2002).
3. S. Nie and R. Emory, "Probing single molecules and single nanoparticles by surface-enhanced Raman scattering," *Science* **275**, 1102 (1997).
4. M. Moskovits, "Surface-enhanced spectroscopy," *Rev. Mod. Phys.* **57**, 783 (1985).
5. S. A. Maier, M. L. Brongersma, P. G. Kik, S. Meltzer, A. A. G. Requicha, and H. A. Atwater, "Plasmonics - A route to nanoscale optical devices," *Adv. Mat.* **13**, 1501 (2001).
6. X. D. Hoa, A. G. Kirk, and M. Tabrizian, "Towards integrated and sensitive surface plasmon resonance biosensors: A review of recent progress," *Biosens. Bioelectron.* **23**, 151-160 (2007).
7. H. R. Stuart and D. G. Hall, "Island size effects in nanoparticle-enhanced photodetectors," *Appl. Phys. Lett.* **73**, 3815 (1998).
8. D. M. Schaadt, B. Feng, and E. T. Yu, "Enhanced semiconductor optical absorption via surface plasmon excitation in metal nanoparticles," *Appl. Phys. Lett.* **86**, 063106 (2005).
9. D. Derkacs, S. H. Lim, P. Matheu, W. Mar, and E. T. Yu, "Improved performance of amorphous silicon solar cells via scattering from surface plasmon polaritons in nearby metallic nanoparticles," *Appl. Phys. Lett.* **89**, 093103 (2006).
10. S. Pillai, K. R. Catchpole, T. Trupke, and M. A. Green, "Surface plasmon enhanced silicon solar cells," *J. Appl. Phys.* **101**, 093105 (2007).
11. S. Pillai, K. R. Catchpole, T. Trupke, G. Zhang, J. Zhao, and M. A. Green, "Enhanced emission from thin Si based LEDs using surface plasmons," *Appl. Phys. Lett.* **88**, 161102 (2006).
12. M. Westphalen, U. Kreibig, J. Rostalski, H. Lüth, and D. Meissner, "Metal cluster enhanced organic solar cells," *Sol. Energy Mater. Sol. Cells* **61**, 97-105 (2000).
13. B. P. Rand, P. Peumans, and S. R. Forrest, "Long-range absorption enhancement in organic tandem thin-film solar cells containing silver nanoclusters," *J. Appl. Phys.* **96**, 7519 (2004).
14. A. J. Morfa, K. L. Rowlen, T. H. Reilly III, M. J. Romero, and J. v. d. Lagemaat, "Plasmon-enhanced solar energy conversion in organic bulk heterojunction photovoltaics," *Appl. Phys. Lett.* **92**, 013504 (2008).
15. R. B. Konda, R. Mundle, H. Mustafa, O. Bamiduro, A. K. Pradhan, U. N. Roy, Y. Cui, and A. Burger, "Surface plasmon excitation via Au nanoparticles in n-CdSe/p-Si heterojunction diodes," *Appl. Phys. Lett.* **91**, 191111 (2007).
16. C. Hägglund, M. Zäch, and B. Kasemo, "Enhanced charge carrier generation in dye sensitized solar cells by nanoparticle plasmons," *Appl. Phys. Lett.* **92**, 013113 (2008).
17. K. R. Catchpole and A. Polman, "Design principles for particle plasmon enhanced solar cells," *Appl. Phys. Lett.* **93**, 191113 (2008).
18. C. F. Bohren and D. R. Huffman, *Absorption and scattering of light by small particles* (Wiley-Interscience, New York, 1983).
19. U. Kreibig and M. Vollmer, *Optical properties of metal clusters*, Springer Series in Materials Science (Springer-Verlag, Berlin, 1995).

20. H. Mertens, A. F. Koenderink, and A. Polman, "Plasmon-enhanced luminescence near noble-metal nanospheres: Comparison of exact theory and an improved Gersten and Nitzan model," *Phys. Rev. B* **76**, 115123 (2007).
21. M. Meier and A. Wokaun, "Enhanced fields on large metal particles: dynamic depolarization," *Opt. Lett.* **8**, 581 (1983).
22. A. Wokaun, J. P. Gordon, and P. F. Liao, "Radiation damping in surface-enhanced Raman scattering," *Phys. Rev. Lett.* **48**, 957 (1982).
23. K. L. Kelly, E. Coronado, L. L. Zhao, and G. C. Schatz, "The optical properties of metal nanoparticles: The influence of size, shape, and dielectric environment," *Journal of Physical Chemistry B* **107**, 668-677 (2003).
24. C. Langhammer, B. Kasemo, and I. Zorić, "Absorption and scattering of light by Pt, Pd, Ag, and Au nanodisks: Absolute cross sections and branching ratios," *J. Chem. Phys.* **126**, 194702 (2007).
25. S. P. Sundararajan, N. K. Grady, N. Mirin, and N. J. Halas, "Nanoparticle-Induced Enhancement and Suppression of Photocurrent in a Silicon Photodiode," *Nano Lett.* **8**, 624-630 (2008).
26. G. Xu, M. Tazawa, P. Jin, S. Nakao, and K. Yoshimura, "Wavelength tuning of surface plasmon resonance using dielectric layers on silver island films," *Appl. Phys. Lett.* **82**, 3811-3813 (2003).
27. H. Mertens, J. Verhoeven, A. Polman, and F. D. Tichelaar, "Infrared surface plasmons in two-dimensional silver nanoparticle arrays in silicon," *Appl. Phys. Lett.* **85**, 1317-1319 (2004).
28. MiePlot, www.philiplaven.com/mieplot.htm.
29. F. Beck, K. R. Catchpole, and A. Polman, "Red-shifting the surface plasmon resonance of silver nanoparticles for light trapping in solar cells," to be published.
30. C. Langhammer, M. Schwind, B. Kasemo, and I. Zoric, "Localized Surface Plasmon Resonances in Aluminum Nanodisks," *Nano Lett.* **8**, 1461-1471 (2008).
31. H. Benisty, R. Stanley, and M. Mayer, "Method of source terms for dipole emission modification in modes of arbitrary planar structures," *J. Opt. Soc. Am. A* **15**, 1192 (1998).
32. B. J. Soller, H. R. Stuart, and D. G. Hall, "Energy transfer at optical frequencies to silicon-on-insulator structures," *Opt. Lett.* **26**, 1421 (2001).
33. J. Mertz, "Radiative absorption, fluorescence, and scattering of a classical dipole near a lossless interface: a unified description," *J. Opt. Soc. Am. B* **17**, 1906 (2000).
34. B. J. Soller and D. G. Hall, "Scattering enhancement from an array of interacting dipoles near a planar waveguide," *J. Opt. Soc. Am. B-Optical Physics* **19**, 2437-2448 (2002).
35. B. Soller, *The Interaction Between Metal Nanoparticle Resonances and Optical Frequency Surface waves* (University of Rochester, 2002).
36. H. R. Stuart and D. G. Hall, "Thermodynamic limit to light trapping in thin planar structures," *J. Opt. Soc. Am. A* **14**, 3001 (1997).
37. K. R. Catchpole and S. Pillai, "Absorption enhancement due to scattering by dipoles into silicon waveguides," *J. Appl. Phys.* **100**, 044504 (2006).
38. K. H. Drexhage, "Influence of a dielectric interface on fluorescence decay time," *J. Lumin.* **1**, 693 (1970).
39. E. Snoeks, A. Lagendijk, and A. Polman, "Measuring and modifying the spontaneous emission rate of erbium near an interface," *Phys. Rev. Lett.* **74**, 2459 (1995).
40. C. Hägglund, M. Zäch, G. Petersson, and B. Kasemo, "Electromagnetic coupling of light into a silicon solar cell by nanodisk plasmons," *Appl. Phys. Lett.* **92**, 053110 (2008).
41. S. H. Lim, W. Mar, P. Matheu, D. Derkacs, and E. T. Yu, "Photocurrent spectroscopy of optical absorption enhancement in silicon photodiodes via scattering from surface plasmon polaritons in gold nanoparticles," *J. Appl. Phys.* **101**, 104309 (2007).

1. Introduction

Photovoltaics has the potential to make a large contribution to solving the problem of climate change. To make electricity from photovoltaics competitive with fossil fuel technologies, the price needs to be reduced by a factor of 2-5 (depending on the local price of electricity generated from fossil fuels). Currently 90 % of the solar cell market is based on crystalline silicon wafers, with thicknesses of 200-300 μm . Around 40% of the cost of a solar module made from crystalline silicon is the cost of the silicon wafers. Because of this, there has been a great deal of research on thin-film solar cells over the past ten years. Thin-film solar cells have thicknesses usually in the range 1-2 μm , and are deposited on cheap substrates such as glass, plastic or stainless steel. They are made from a variety of semiconductors including cadmium telluride and copper indium diselenide, as well as amorphous and polycrystalline silicon. A major limitation in all thin film solar cell technologies is that their absorbance of near-bandgap light is ineffective, in particular for the indirect-bandgap semiconductor silicon. Therefore, structuring the solar cell so that light is trapped inside, in order to increase the absorbance, is very important.

Because silicon is a weak absorber, light-trapping is also used in wafer-based cells. For wafer cells, pyramids with a size of 2-10 μm are etched into the surface. For thin-film cells with thicknesses in the micron range, surface texturing with these dimensions is not suitable, so new methods must be found. It is possible to achieve light-trapping by forming a wavelength-scale texture on the substrate and then depositing the thin-film solar cell on top, and large increases in photocurrent have been achieved in this way [1, 2]. However, a rough semiconductor surface results in increased surface recombination, and semiconductors deposited on rough surfaces typically have low material quality.

A new method for increasing the light absorption that has emerged recently is the use of scattering from noble metal nanoparticles excited at their surface plasmon resonance. In this paper we review recent progress in this field and discuss the basic mechanisms involved and potential for improvement.

2. State of the art

The optical properties of metal particles have been studied since the time of Faraday. In recent decades interest has intensified, in particular due to the discovery that Raman scattering can be increased by orders of magnitude through the use of metal nanostructures [3, 4]. Following this, there has been a great deal of work in fundamental properties and applications of plasmonic resonances, especially in integrated optics and biosensing [5, 6].

Pioneering work in the area of plasmonic enhancement of light-sensitive devices was done by Stuart and Hall, who showed that an enhancement in the photocurrent of a factor of 18 could be achieved for a 165 nm thick silicon-on-insulator photo-detector at a wavelength of 800nm using silver nanoparticles on the surface of the device [7]. Subsequently Schaadt *et al.* deposited gold nanoparticles on highly doped wafer-based solar cells, obtaining enhancements of up to 80% at wavelengths around 500nm [8]. Derkacs *et al.* used Au nanoparticles on thin-film amorphous silicon solar cells to achieve an 8 % overall increase in conversion efficiency [9]. Recently, Pillai *et al.* deposited silver particles on 1.25 μm thick silicon-on-insulator solar cells and planar wafer based cells, and achieved overall photocurrent increases of 33 % and 19 % respectively [10]. By reciprocity, metal nanoparticles can also be used to increase the light extraction efficiency of light-emitting diodes and indeed, Pillai *et al.* have reported an overall electroluminescence enhancement of a factor of 7 for thin silicon-on-insulator light-emitting diodes [10, 11].

Enhancements due to particle plasmons have also been reported for other semiconductors than silicon. Here, early work was done by Stenzel *et al.*, who reported an enhancement in photocurrent by up to a factor of 2.7 for ITO-copper phthalocyanine-indium structures. Westphalen *et al.* reported an enhancement for silver clusters incorporated in an ITO and zinc phthalocyanine solar cell [12]. Rand *et al.* have reported enhanced efficiencies for ultra-thin film organic solar cells due to the presence of very small (5 nm diameter) silver nanoparticles [13]. Morfa *et al.* have reported an increase in efficiency by a factor of 1.7 for organic bulk heterojunction solar cells [14]. Increased photocurrent has also been reported for CdSe/Si heterostructures [15] and enhanced carrier generation has been observed in dye-sensitized TiO₂ films [16]. Most recently, we have shown theoretically that particle shape is a crucial parameter determining the light trapping efficiency: path length enhancements in thin films of up to a factor of 30 were found for optimized shapes [17].

3. Basic mechanisms

Two main basic mechanisms have been proposed to explain photocurrent enhancement by metal particles incorporated into or on solar cells: light scattering and near-field concentration of light. The contribution of each mechanism depends mostly on the particle size, how strongly the semiconductor absorbs and the electrical design of the solar cell. This paper focuses on scattering by metal particles as a means to enhance light trapping into thin-film solar cells because it is the mechanism behind the enhancement in most of the experimental work that has been reported.

4. Light scattering by metal particles

Metal nanoparticles are strong scatterers of light at wavelengths near the plasmon resonance, which is due to a collective oscillation of the conduction electrons in the metal. For particles with diameters well below the wavelength of light, a point dipole model describes the absorption and scattering of light well. The scattering and absorption cross-sections are given by [18]:

$$C_{scat} = \frac{1}{6\pi} \left(\frac{2\pi}{\lambda} \right)^4 |\alpha|^2, \quad C_{abs} = \frac{2\pi}{\lambda} \text{Im}[\alpha] \quad (1)$$

where

$$\alpha = 3V \left[\frac{\epsilon_p / \epsilon_m - 1}{\epsilon_p / \epsilon_m + 2} \right] \quad (2)$$

is the polarizability of the particle. Here V is the particle volume, ϵ_p is the dielectric function of the particle and ϵ_m is the dielectric function of the embedding medium. We can see that when $\epsilon_p = -2\epsilon_m$ the particle polarizability will become very large. This is known as the surface plasmon resonance. At the surface plasmon resonance the scattering cross-section can well exceed the geometrical cross section of the particle. For example, at resonance a small silver nanoparticle in air has a scattering cross-section that is around ten times the cross-sectional area of the particle. In such a case, to first-order, a substrate covered with a 10 % areal density of particles could fully absorb and scatter the incident light. For light trapping it is important that scattering is more efficient than absorption, a condition that is met for larger particles, as follows from Eq. (1). Typically, a Ag particle with a diameter of 100 nm has an albedo (scattering cross section over sum of scattering and absorption cross sections) that exceeds 0.9. At these larger sizes, dynamic depolarization and radiation damping become important corrections to the quasi-static expressions given in Eqs. (1) and (2). Furthermore, for larger size the excitation higher-order plasmon modes (quadrupole, octupole) must be taken into account [18-20].

Dynamic depolarization occurs because as the particle size increases, conduction electrons across the particle no longer move in phase. This leads to a reduction in the depolarization field (which is generated by the surrounding polarized matter) at the centre of the particle [21]. As a result, there is a reduced restoring force and hence a red-shift in the particle resonance. For particle sizes where scattering is significant, this re-radiation leads to a radiative damping correction to the quasi-static polarizability, the effect of which is to significantly broaden the plasmon resonance [22]. The red-shift and broadening of the resonance with increased particle size would generally be expected to be an advantage for solar cell applications, since light-trapping should occur over a relatively broad wavelength range and at wavelengths that are long compared with the quasi-static values of the surface plasmon resonance wavelengths of noble metal particles. While an increased size leads to a larger absolute scattering cross section, these effects do lead to a reduced cross section when normalized by size. Inclusion of dynamic depolarization and radiative damping effects can give reasonably accurate predictions of many features of the extinction spectra for larger particles for cases where the contribution of higher order multipoles can be neglected [23, 24].

Particle shape also plays an important role in the effect of metal nanoparticles on a photovoltaic device. Particle shapes such as disks that have a large fraction of their volume close to the semiconductor can lead to a very high fraction of light scattered into the substrate [17]. Conversely, Sundararajan et al. have shown that nanoparticle aggregates can lead to a reduction of photocurrent, a point that must be considered in colloidal fabrication of

nanoparticle assemblies [25]. They have also shown that nanoshells can lead to optical vortexing, which resulted in a reduction in photo-generated current.

For metals with low interband absorption, the dielectric function can be described by the Drude model, which describes the response of damped, free electrons to an applied electromagnetic field of angular frequency ω :

$$\varepsilon = 1 - \frac{\omega_p^2}{\omega^2 + i\gamma\omega} \quad (3)$$

Here ω_p is the bulk plasmon frequency, given by $\omega_p^2 = Ne^2 / m\varepsilon_0$, where N is the density of free electrons, e is the electronic charge, m is the effective mass of an electron and ε_0 is the free-space dielectric constant. Inserting Eq. (3) in Eq. (2) leads to (in free space)

$$\alpha = 3V \frac{\omega_p^2}{\omega_p^2 - 3\omega^2 - i\gamma\omega} \quad (4)$$

Thus the surface plasmon resonance frequency for a sphere in free space occurs at $\omega_{sp} = \sqrt{3}\omega_p$ and mainly depends on the density of free electrons in the particle. The density of free electrons is highest for aluminum and silver, leading to surface plasmon resonances in the ultra-violet, and lower for gold and copper, leading to surface plasmon resonances in the visible. The resonance frequency can be tuned by varying the dielectric constant of the embedding medium: a higher index leads to a red-shift of the resonance [26, 27].

Figure 1 shows scattering and extinction (scattering plus absorption) cross-sections for 100-nm diameter Ag spheres embedded in air, silicon nitride and silicon, calculated with Mie theory [18, 28], using the Drude model fitted to experimental data as input for the dielectric constants. Cross sections are normalized to the geometrical particle cross section. For each embedding medium, a dipole resonance is observed, peaking at 390 nm for air, 690 nm for Si_3N_4 and 1190 nm (outside the wavelength range of Fig. 1) for Si. Shorter wavelength quadrupole, octupole (and in the case of silicon, hexadecapole) resonances are also observed. Comparing the scattering and extinction spectra, it can be seen that the higher-order multipole resonances exhibit slightly lower albedo but still shows significant scattering cross sections. The shift of the plasmon resonance with local dielectric environment and the contribution of higher order multipoles needs to be considered for all solar cell geometries, but in particular for proposals to put metal nanoparticles within the active layers of solar cells. (For such proposals it would also be important to ensure that the semiconductor was well passivated to avoid very rapid recombination of electron-hole pairs at the metal-semiconductor interface). The effectiveness of varying the underlying dielectric on tuning the photocurrent enhancement spectrum has been experimentally and numerically demonstrated by Beck *et al.* [29]. It is interesting to note that in the infrared wavelength range desired for most light trapping applications, beyond 700 nm, the dielectric functions of Au and Ag are very similar [17]. Ag, due its lower absorption and lower cost is thus a better choice than Au, although it must be well encapsulated to avoid oxidation effects that are not present for Au. Cu is cheaper but is even more absorbing than Au. For Al the effects of the interband transition at 1.5eV and the native oxide on the scattering cross-section and albedo would need to be considered [30].

For light trapping applications, the metal nanoparticles are placed on a semiconductor substrate, and light is preferentially scattered into the high-index substrate. The angular scattering distribution of a dipole on a dielectric substrate can be calculated with a number of methods [31-33]. We focus here on the method of Mertz [33], which allows calculation of scattering cross-sections as well as radiation patterns in lossless substrates. While in a true light trapping application, absorption in the semiconductor substrate must clearly be taken into account, this method provides clear physical insights.

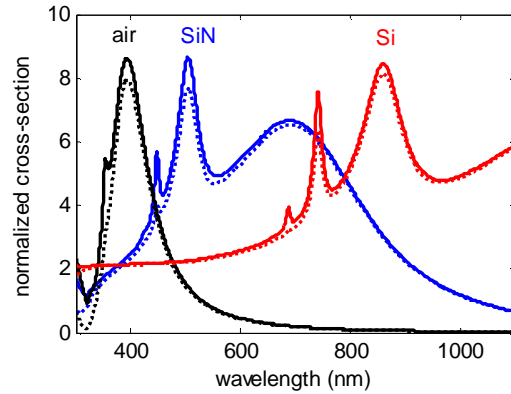


Fig. 1. Extinction (solid lines) and scattering (dashed lines) cross-sections for 100-nm diameter Ag spheres embedded in air (black), Si_3N_4 ($n=2$, blue) and Si (red), normalized by the projected area of the sphere. The dipolar resonance for Si peaks at 1190 nm and is outside the range of the graph.

Figure 2(a) shows a polar plot of the radiation pattern for an electric dipole with a dipole moment parallel to the surface, placed 20 nm above a (lossless) substrate with index 3.5. The radiation pattern for an electric dipole in free space is plotted for reference. We can see that for the dipole above a silicon surface, only a tiny, barely visible, fraction of the light is radiated into the air, while the vast majority (96 %) is radiated into the silicon. The effectiveness of this transfer of energy from a dipole to a high index substrate has been pointed out by Soller *et al.* [32], and is related to the high density of optical modes within the silicon. The angular distribution also shows that a significant fraction of the light is coupled into the Si at an angle exceeding the critical angle of 16° . This is because light scattered with high in-plane wave-vectors, that are evanescent in air, can propagate in silicon. Figure 2(b) shows radiation patterns of dipoles placed at 20 nm and 60 nm from the substrate, respectively. We can see that at larger distances from the substrate, a reduced fraction of the light is radiated into the substrate (e.g. 84 % for a dipole 60 nm from the substrate). We can also see that the fraction of light coupled outside the critical angle decreases as the distance from the dipole to the substrate decreases.

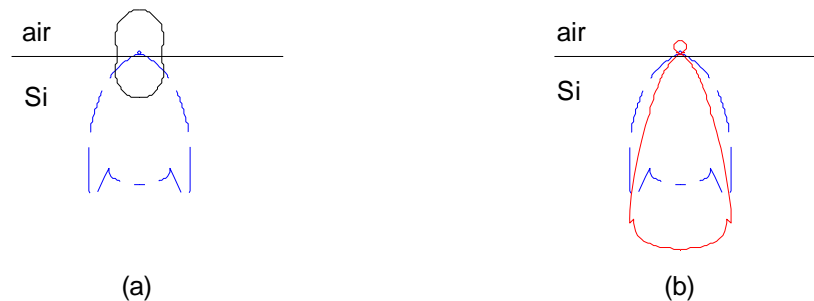


Fig. 2. (a) Radiation patterns for a point dipole oriented parallel to the surface at a distance of 20 nm from a Si substrate (blue dashed line). The radiation pattern for the case of free space is shown for reference (black solid line). (b) Radiation patterns for a parallel point dipole 20 nm (blue dashed line) and 60 nm (red solid line) from a Si substrate.

The fraction of light scattered into thick semiconductor devices and thin (eg. SOI) waveguides is high for the same reason in each case, which is the very high density of optical modes in the

semiconductor compared to air. In the case of waveguides the fraction scattered into the waveguide is higher for wavelengths where an optical mode nears cut-off. This is because near cut-off the evanescent field associated with an optical mode extends further beyond the waveguide, so interaction with a nanoparticle located within the evanescent field is increased [34, 35]. However, it is also important to note that for waveguides with only a few optical modes, the reduced density of optical modes compared to a thick substrate will also tend to reduce the fraction of light scattered into the waveguide [36].

In addition to the changes in radiation pattern, the scattering cross-section is also altered by the presence of a substrate. Figure 3 (right-hand axis) shows a plot of the scattering cross-section for a point dipole above a Si substrate, at the dipole resonance, assuming no Ohmic losses. Light is incident at normal incidence, and the scattering cross section is plotted relative to the cross-section in the absence of the substrate. The decrease in relative scattering cross-section close to the substrate is due to the reduced driving field due to interference of the incident and reflected fields. For a waveguide substrate there will be both increases and decreases to the scattering cross-section, depending on the wavelength [37]. In realistic cases, with metal nanoparticles that exhibit Ohmic losses, the normalized scattering cross section is further modulated due to variations of the local optical density of states near the interface [38, 39].

Figure 3 also shows the fraction of fraction of light that is scattered into the substrate for a point dipole as a function of distance from the substrate. As seen in Fig. 2, the scattered fraction decreases with distance. The overall effect of varying distance is thus a tradeoff between increase cross section and reduced coupled fraction [17]. The optimum distance is then determined by the absorption co-efficient of the semiconductor layer, the desired particle density (which is related to the cross section) and the degree of Ohmic loss in the particles. We note that, as seen in Fig. 1, Ag nanoparticles embedded in Si show interesting higher-order plasmon resonances with high albedo. These higher-order modes do show reduced coupling into a dielectric substrate because the field around the particle decays much faster than for the dipolar resonance [40].

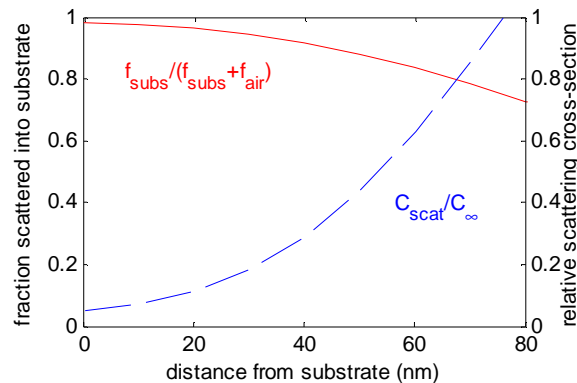


Fig. 3. Normalized scattering cross section for light scattered from a point-dipole into a Si substrate, as a function of distance to the substrate (blue dashed line). Also plotted is the fraction of light scattered into the substrate as a function of distance (red solid line).

For excitation at wavelengths below the resonance the scattered radiation is out of phase with the incident radiation (see Eqn. (4)), the phase difference depending on the frequency, and as a result the scattered light interferes destructively with the direct (non-scattered) incident light [18]. This leads to reduced coupling of light into the semiconductor and consequently a reduced photocurrent for wavelengths below the resonance wavelength [41]. Thus the maximum in-coupling and maximum photo-current occurs slightly above the surface plasmon

resonance wavelength, where the scattering cross-section is high but the scattered field is still approximately in phase with the incident field. In Fig. 3 the effect of phase has been removed to allow the factors affecting the overall enhancement to be assessed separately. To obtain the overall enhancement the fraction of light scattered into the substrate would need to be combined with the scattering cross-section and phase information. However, because the phase changes only slowly with wavelength until very close to the resonance, the fraction of light scattered into the substrate will give a good approximation to the fraction of the total intensity in the substrate up to around the position of the maximum in photocurrent.

5. Conclusions and outlook

Localized surface plasmons have been shown to provide substantial efficiency enhancement in solar cells with a range of semiconducting materials and device and particle geometries. This paper reviewed many of the basic concepts behind light scattering from metal nanoparticles on a dielectric substrate. Much more work remains to be done to determine the optimum particle distribution for solar cell applications, taking into account interactions between the particles as well as including the interaction with the absorbing substrate in a realistic way. We note that relatively simple and inexpensive methods for fabricating such nanostructured metal patterns over large areas, using soft lithography, are already available.

Acknowledgments

This work is part of the research program of the "Stichting voor Fundamenteel Onderzoek der Materie (FOM)", which is financially supported by the "Nederlandse organisatie voor Wetenschappelijk Onderzoek (NWO)". It is part of an Industrial Partnership Program between FOM and the Foundation Shell Research. Dr. Catchpole is the recipient of an Australian Research Council Fellowship (project DP0880017).